VOLS. 159–160 • 15 March 2009 • ISSN 0921-5107
Complete in two Volumes

ELSEVIER

MATERIALS SCIENCE & ENGINEERING

B Advanced Functional Solid-state Materials

Editor-in-Chief:
P.N. Kumta

Deputy Editor:
D. Schleich

Founding Editors:
M. Balkanski
H. Kamimura
S. Mahajan

Special Issue:
EMRS 2008 Spring Conference Symposium K: Advanced Silicon Materials Research for Electronic and Photovoltaic Applications

Guest Editors:
S. Pizzini, G. Kissinger, H.Tu, H.Yamada-Kaneta

Available online at www.sciencedirect.com
ScienceDirect

Materials Science and Engineering B 159–160 (2009) 149–152

Contents lists available at ScienceDirect

Materials Science and Engineering B

journal homepage: www.elsevier.com/locate/mseb

Molecular dynamics simulation of defect formation and precipitation in heavily carbon doped silicon

F. Zirkelbach[a,*], J.K.N. Lindner[a], K. Nordlund[b], B. Stritzker[a]

[a] *Experimentalphysik IV, Institut für Physik, Universität Augsburg, Universitätsstr. 1, D-86135 Augsburg, Germany*
[b] *Accelerator Laboratory, Department of Physical Sciences, University of Helsinki, Pietari Kalmink. 2, 00014 Helsinki, Finland*

ARTICLE INFO

Article history:
Received 10 May 2008
Received in revised form 2 October 2008
Accepted 9 October 2008

Keywords:
Silicon
Carbon
Silicon carbide
Nucleation
Defect formation
Molecular dynamics simulations

ABSTRACT

The precipitation process of silicon carbide in heavily carbon doped silicon is not yet fully understood. High resolution transmission electron microscopy observations suggest that in a first step carbon atoms form C—Si dumbbells on regular Si lattice sites which agglomerate into large clusters. In a second step, when the cluster size reaches a radius of a few nm, the high interfacial energy due to the SiC/Si lattice misfit of almost 20% is overcome and the precipitation occurs. By simulation, details of the precipitation process can be obtained on the atomic level. A recently proposed parametrization of a Tersoff-like bond order potential is used to model the system appropriately. Preliminary results gained by molecular dynamics simulations using this potential are presented.

1. Introduction

Understanding the precipitation process of cubic silicon carbide (3C—SiC) in heavily carbon doped silicon will enable significant technological progress in thin film formation of the important wide band gap semiconductor material SiC [1]. On the other hand it will likewise offer perspectives for processes which rely upon prevention of precipitation events, e.g. the fabrication of strained, pseudomorphic $Si_{1-y}C_y$ heterostructures [2].

Epitaxial growth of 3C—SiC films is achieved either by ion beam synthesis (IBS) [3], chemical vapour deposition (CVD) or molecular beam epitaxy (MBE) techniques. While in CVD and MBE surface effects need to be taken into account, SiC formation during IBS takes place in the bulk of the Si crystal. In the present work the simulation assumes conditions similar to those of the ion implantation process.

First of all a picture of the supposed precipitation event is presented. Then the applied simulation sequences are introduced. Finally preliminary simulation results are presented.

2. Supposed Si to 3C—SiC conversion mechanism

Crystalline silicon (c-Si) has diamond structure and thus is composed of two fcc lattices which are displaced by one quarter of the volume diagonal. 3C—SiC grows in zincblende structure, i.e. is also composed of two fcc lattices, one out of which is occupied by Si and the other by C atoms. The length of four lattice constants of c-Si is approximately equal to the length of five 3C—SiC lattice constants ($4a_{\text{Si}} \approx 5a_{\text{3C–SiC}}$) resulting in a lattice misfit of almost 20%. Due to this the silicon atomic density of 3C—SiC is slightly lower than the one of c-Si.

There is a supposed conversion mechanism of heavily carbon doped c-Si into 3C—SiC [4]. As concluded from high resolution transmission electron microscopy (HREM) carbon atoms introduced into c-Si form C—Si dumbbells on regular Si lattice sites. The dumbbells agglomerate into large clusters, called embryos. Finally, when the cluster size reaches a critical radius of 2–4 nm, the high interfacial energy due to the 3C—SiC/c-Si lattice misfit is overcome and precipitation occurs. In HREM this transformation manifests itself by the disappearance of patches with dark background in favor of high resolution Moiré fringes due to 3C—SiC precipitates embedded in c-Si [3,4]. Due to the slightly lower silicon density of 3C—SiC excessive silicon atoms exist, which will most probably end up as self-interstitials in the c-Si matrix since there is more space than in 3C—SiC.

Thus, in addition to the precipitation event itself, knowledge of C and Si interstitials in Si are of great interest in order to investigate the precipitation of 3C—SiC in heavily C doped c-Si.

3. Simulation sequences

A molecular dynamics simulation approach is used to examine the steps involved in the precipitation process. For integrating

---

[*] Corresponding author. Tel.: +49 821 5983008; fax: +49 821 5983425.
E-mail address: frank.zirkelbach@physik.uni-augsburg.de (F. Zirkelbach).

0921-5107/$ – see front matter © 2008 Elsevier B.V. All rights reserved.
doi:10.1016/j.mseb.2008.10.010

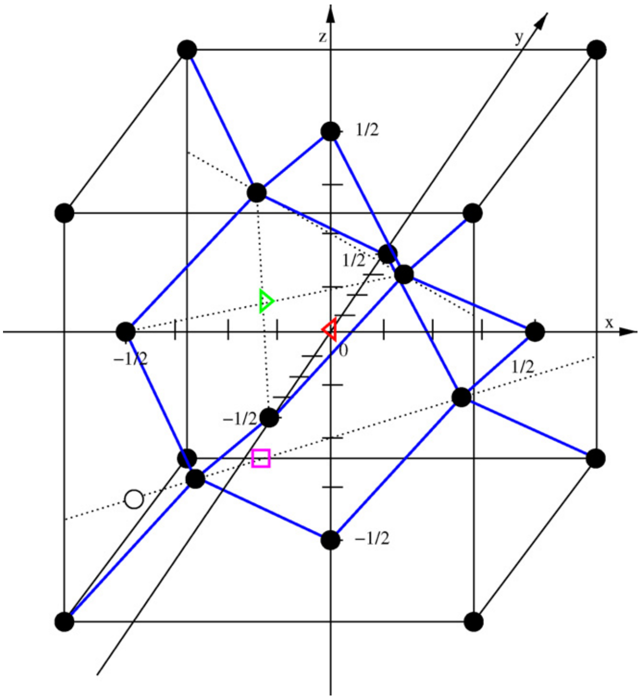

Fig. 1. Insertion positions for the tetrahedral (◁), hexagonal (▷) and $\langle 1\,1\,0\rangle$ dumbbell (□) interstitial configuration.

the equations of motion the velocity verlet algorithm [5] with a timestep of 1 fs is adopted. The interaction of the silicon and carbon atoms is realized by a newly parametrized Tersoff-like bond order potential [6]. Since temperature and pressure of the system is kept constant in experiment the isothermal–isobaric NPT ensemble is chosen for the simulation. Coupling to the heat bath is achieved by the Berendsen thermostat [8] with a time constant of 100 fs. The pressure is controlled by the Berendsen barostat [8] again using a time constant of 100 fs and a bulk modulus of 100 GPa for silicon. To exclude surface effects periodic boundary conditions are applied. In order to study the behaviour of carbon in c-Si, two different simulation sequences are used.

To investigate the interstitial configurations of C and Si atoms in c-Si, a simulation volume of $9 \times 9 \times 9$ silicon unit cells is used. The temperature is set to 0 K. In separated simulation runs a carbon or a silicon atom is inserted in the central unit cell at the tetrahedral $(0, 0, 0)$ (◁), a hexagonal $(-1/8, -1/8, 1/8)$ (▷), a nearly dumbbell $(-1/8, -1/8, -1/4)$ (□) or at a random position (in units of the silicon lattice constant) where the origin is located in the centre of the unit cell (Fig. 1). In order to avoid too high potential energies in the case of the dumbbell configuration the nearest silicon neighbour atom is manually shifted to $(-3/8, -3/8, -1/4)$ ($\circ$). The energy introduced into the system by the insertion of atoms is scaled out within a relaxation phase of 2 ps.

For the simulations aiming to reproduce a precipitation process the simulation volume is 31 silicon lattice constants in each direction. The system temperature is set to 450 °C like in IBS [3]. 6000 carbon atoms (the number necessary to form a 3C—SiC precipitate with a radius of ~ 3 nm) are consecutively inserted in a way to keep the system temperature constant. Carbon is inserted statistically distributed over either the whole simulation volume (insertion volume V_1), an insertion volume V_2 corresponding to the minimum size of a 3C—SiC precipitate or the volume V_3 containing the number of Si atoms necessary for the formation of such a minimum precipitate. The two latter insertion volumes are considered since no diffusion of carbon atoms is observed at this temperature. The absence of carbon diffusion even at elevated temperatures might be attributed to unphysical high forces necessary to split the Si—C bonds. These forces are introduced by the sharp cut-off function used in the short-range potential [7]. Following the insertion procedure the system is cooled down to 20 °C.

4. Results

The insertion of individual Si atoms leads to stable tetrahedral and $\langle 1\,1\,0\rangle$ dumbbell self-interstitial configurations as observed earlier in [6]. The formation energies are 3.4 eV and 4.4 eV, respectively. However, the hexagonal dumbbell configuration is not stable opposed to results in [6]. The Si interstitial atom moves towards an energetically more favorable position very close to the tetrahedral one but slightly displaced along the three coordinate axes. The formation energy of 4.0 eV for this type of interstitials equals the result obtained in [6] for the hexagonal one. The same type of interstitial arises using random insertions. In addition, variations exist in which the displacement is only along two $\langle 1\,0\,0\rangle$ axes ($E_f = 3.8$ eV) or along a single $\langle 1\,0\,0\rangle$ axis ($E_f = 3.6$ eV) successively approximating the tetrahedral configuration and formation energy.

In carbon insertion simulations the tetrahedral and $\langle 1\,1\,0\rangle$ dumbbell carbon interstitial configurations are observed to be stable. The formation energies are 2.7 eV and 1.8 eV, respectively. Again, the hexagonal configuration is found to be unstable. The carbon interstitial atom moves to the more favorable $\langle 1\,0\,0\rangle$ dumbbell position which has a formation energy of 0.5 eV. There is experimental [9] and theoretical [10] evidence of the existence of this configuration. It is frequently generated and has the lowest formation energy of all the defects observed in all the simulation runs in which carbon is inserted at random positions. Fig. 2 schematically displays the $\langle 1\,0\,0\rangle$ dumbbell configuration including the atomic displacements relative to the atoms initial positions together with resulting new Si—Si and C—Si pair distances.

Fig. 3 shows resulting pair correlation functions of the simulation runs targeting the observation of precipitation events. The contributions of Si—C and C—C pairs are presented separately. The three curves represent results for the insertion of 6000 C atoms into the three different volumes V_1, V_2 and V_3, as explained above. There is no significant difference between carbon insertions into V_2 and V_3.

The number of C—C bonds for V_1 is much smaller than for V_2 and V_3 since carbon atoms are spread over the total simulation volume, which means that there is only 0.2 carbon atoms per silicon unit cell on average. The first C—C peak appears at about 0.15 nm. This is comparable to the nearest neighbour distance of graphite or diamond. It is assumed that these carbon atoms form strong C—C bonds which is supported by a decrease of the total energy during carbon insertion for the V_2 and V_3 in contrast to the V_1 simulation.

The C—C peak at ~ 0.31 nm perfectly matches the distance of two carbon atoms in the 3C—SiC lattice. In 3C—SiC the same distance is also expected for Si—Si bonds. The Si—Si portion of the pair correlation function for the case of 3000 C atoms inserted into V_2 is displayed in Fig. 4, together with a reference function for pure c-Si. After insertion of C atoms the Si—Si pair correlation function in fact shows non-zero $g(r)$ values around distance values of 0.31 nm while the amount of Si pairs at the regular distances of 0.24 nm and 0.38 nm decreases. However, no clear peak is observed but the interval of enhanced $g(r)$ values corresponds to the width of the C—C $g(r)$ peak. Analyses of randomly chosen configurations in which distances around 0.3 nm appear, identify $\langle 1\,0\,0\rangle$ C—Si dumbbells to be responsible for stretching the Si—Si next neighbour distance for low C concentrations, i.e. for the V_1 and early stages of V_2 and V_3 simulation runs. This excellently agrees with the cal-

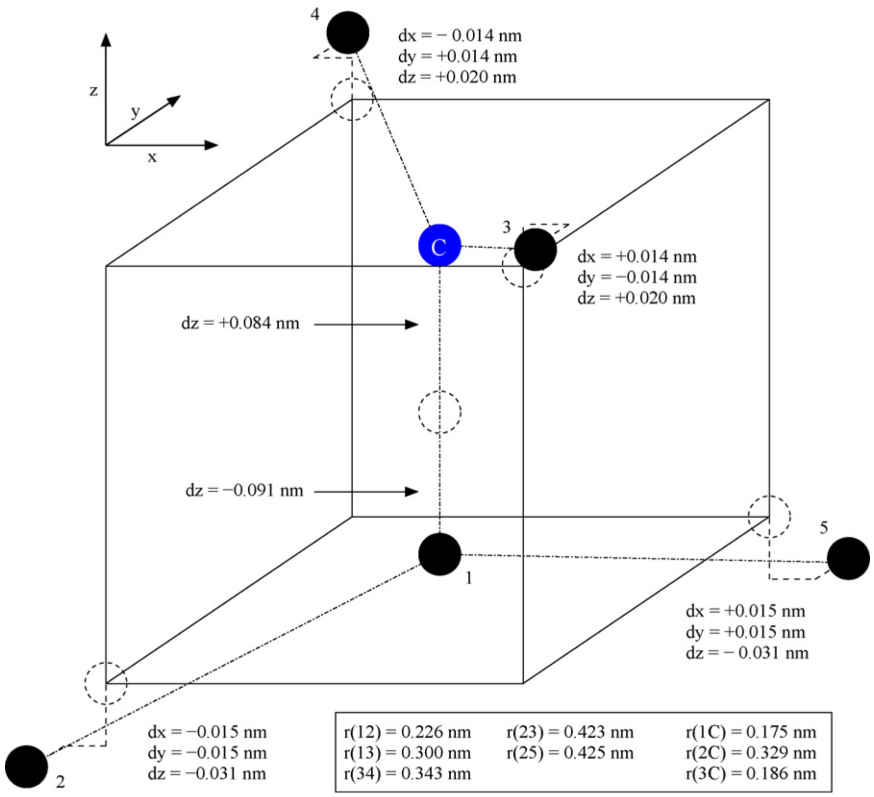

Fig. 2. Schematic of the ⟨1 0 0⟩ C—Si dumbbell configuration. Displacements of the atoms relative to their initial position are given. The displacement of the carbon atom is relative to the initial position of atom 1. New resulting Si—Si and C—Si pair distances $r(ij)$ for the atoms (ij) shown in the schematic are recorded.

culation for a single ⟨1 0 0⟩ dumbbell ($r(13)$ in Fig. 2). For higher C concentrations the defect concentration is likewise increased and a considerable amount of damage is introduced into the insertion volume. Damage and superposition of defects generate new displacement arrangements which become hard to categorize and trace and obviously lead to a broader distribution of pair distances. The step-like increase of Si—Si pairs at 0.29 nm is probably due to the Si—Si cut-off radius of 0.296 nm in the used bond order potential [6]. The cut-off function causes artificial forces pushing the Si atoms out of the cut-off region. By visualizing the C—C atom pairs with distances of 0.31 nm, concatenated, differently oriented ⟨1 0 0⟩ dumbbell interstitials are frequently observed. Indeed this configurations was already reported in [10]. This leads to the assumption that C atoms introduced in that way are the first elements arranged at distances expected for 3C—SiC which at a later stage pull the Si atoms into the right configuration.

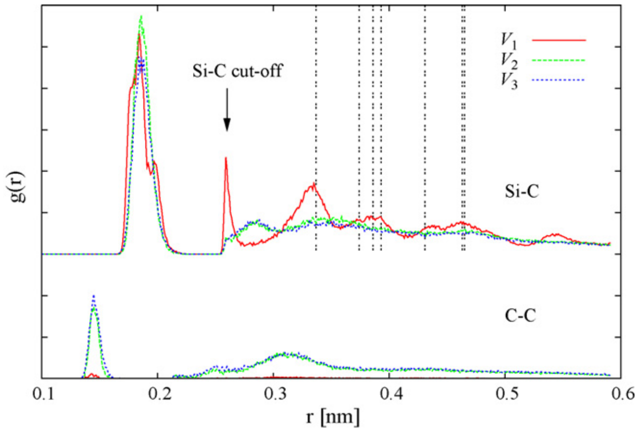

Fig. 3. Pair correlation functions for Si—C and C—C bonds. The three curves represent results for the three different insertion volumes V_1, V_2 and V_3, as explained in the text. The dashed vertical lines mark further calculated C—Si atom pair distances appearing in the ⟨1 0 0⟩ C—Si dumbbell interstitial configuration, which are not displayed in Fig. 2.

The Si—C pair correlation (Fig. 3) shows the formation of Si—C atom pairs displaced approximately by 0.187 nm. This corresponds quite well to the expected next neighbour distance of 0.189 nm for Si and C atoms in 3C—SiC. For low concentrations again ⟨1 0 0⟩ dumbbell configurations can be identified to contribute to this pair distance ($r(3C)$ in Fig. 2). Further more, the bump at 0.175 ($r(1C)$ in Fig. 2) and the peaks at about 0.333 nm, 0.374 nm, 0.386 nm, 0.431 nm and 0.464 nm are comprehensible by comparing with

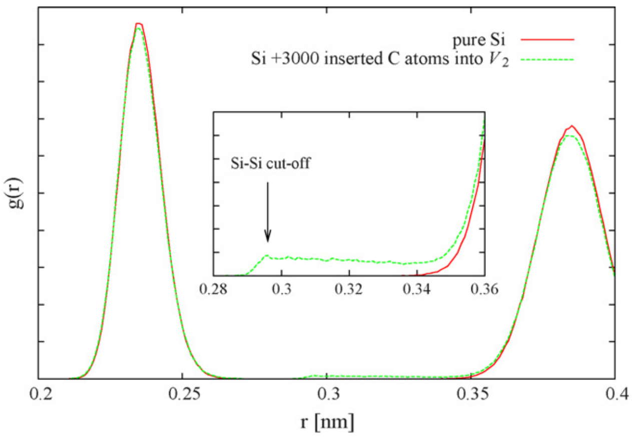

Fig. 4. Si—Si pair correlation function for pure Si and Si with 3000 inserted C atoms. The inset shows a magnified region between 0.28 nm and 0.36 nm.

calculated values in Fig. 2 and the dashed vertical lines in Fig. 3. The dashed lines mark further calculated C—Si atom pair distances appearing in the ⟨1 0 0⟩ C—Si dumbbell interstitial configuration which are not displayed in Fig. 2. The distinct peak at 0.26 nm, which exactly matches the cut-off radius of Si—C interaction, is again a potential artefact. For high carbon concentrations again superposition of defects and high amounts of damage characterize the pair distances. Short range order indeed is observed but only hardly visible is the long range order, which indicates the formation of an amorphous SiC-like phase. This suggests to use higher temperatures instead of longer time scales not accessible to simulation, particularly with regard to V_2 and V_3 simulations, i.e. simulations with high carbon concentrations. This could help the system to get over an energy barrier escaping a local minimum configuration to transform into the crystalline phase.

5. Summary

The conversion of heavily C doped c-Si into 3C—SiC precipitates is investigated. Molecular dynamics simulation sequences to analyze interstitial configurations and the precipitation of 3C—SiC are introduced. The ⟨1 0 0⟩ C—Si dumbbel reproduced by simulation is observed the energetically most favorable configuration and explained in detail. First results of the simulations suggest that in the precipitation process C atoms introduced as differently oriented C—Si dumbbells into the c-Si matrix are the first elements properly arranged for the 3C—SiC formation. Furthermore, the observation of high amounts of damage particularly for high carbon concentrations demands for elevated system temperatures to achieve the precipitation event.

References

[1] J.H. Edgar, J. Mater. Res. 7 (1992) 235.
[2] J.W. Strane, S.R. Lee, H.J. Stein, S.T. Picraux, J.K. Watanabe, J.W. Mayer, J. Appl. Phys. 79 (1996) 637.
[3] J.K.N. Lindner, Appl. Phys. A 77 (2003) 27.
[4] P. Werner, R. Koegler, W. Skorupa, D. Eichler, in: E. Ishidida, S. Banerjee, S. Mehta, T.C. Smith, M. Current, L. Larson, A. Tasch, T. Romig (Eds.), Proceedings of the 11th International Conference on Ion Implantation Technology, Austin, TX, USA, June 16–21, 1996, p. 675.
[5] L. Verlet, Phys. Rev. 159 (1967) 98.
[6] P. Erhart, K. Albe, Phys. Rev. B 71 (2005) 35211.
[7] A. Mattoni, M. Ippolito, L. Colombo, Phys. Rev. B 76 (2007) 224103.
[8] H.J.C. Berendsen, J.P.M. Postma, W.F. van Gunsteren, A. DiNola, J.R. Haak, J. Chem. Phys. 81 (1984) 3684.
[9] G.D. Watkins, K.L. Brower, Phys. Rev. Lett. 36 (1976) 1329.
[10] A. Mattoni, F. Bernardini, L. Colombo, Phys. Rev. B 66 (2002) 195214.